

# Rare Earth doped $\text{LaPO}_4$ Phosphor Synthesis and Characterization

S. Kondala Rao<sup>1</sup>, P. Indira<sup>2</sup> and K. V. R. Murthy<sup>3</sup>

<sup>1</sup>Department of Physics, QIS College of Engineering and Technology, Ongole-523001, India

<sup>2</sup>Department of Physics, Sri ABR Government Degree College, Repalle-, India

<sup>3</sup>Display Materials Laboratory, Applied Physics Department, Faculty of Technology & Engineering, M.S University of Baroda, Baroda-390001, India

Email: [sayana.1980@gmail.com](mailto:sayana.1980@gmail.com)

## ABSTRACT

The present paper reports the Synthesis and Photoluminescence (PL) studies of the  $\text{LaPO}_4$  phosphor doped with Eu (0.5), Tb (1.0) and Ce with 0.5, 1.0, 1.5, 2.0, 3.0, 4.0 and 5.0 mole percentages respectively. The phosphor was synthesized using the standard solid state diffusion reaction technique. The mixture was fired at 1200°C for 3 hours with heating rate of 5°C/min in a muffle furnace and the received cake is ground using mortar and pestle. The powder phosphors were characterized by X-ray diffraction, FTIR and scanning electron microscopy. The crystallinity and phase purity of the phosphor was confirmed by XRD studies. The Infrared spectra for the prepared solid nano powders were recorded in the range between 400 and 4000  $\text{cm}^{-1}$  on a Fourier transform spectrometer. The particle morphology of the phosphor was characterized by SEM. The Photoluminescence properties of the materials were studied using Spectrofluorophotometer at room temperature. The Photoluminescence (PL) excitation spectra were recorded for different excitation wavelengths at 254 nm, 264 nm and 275 nm monitoring at 614 and 545nm. The PL emission of Eu(0.5), Tb(1.0) and Ce(0.5, 1.0, 1.5, 2.0, 3.0, 4.0 and 5.0 mol%) doped  $\text{LaPO}_4$  phosphor was recorded for different excitation wavelengths. The PL emission peaks are found at 364, 381, 415, 438, 470, 488, 545, 589, 594, 614 and 622nm with good intensity.

**Keywords:** Photoluminescence [PL], Rare Earth ions [RE ions], XRD, Solid State Reaction [SSR].

## 1. INTRODUCTION:

Recently various phosphors like  $\text{LaPO}_4$ : Ce, Tb has been good commercial green phosphor materials have been actively investigated to improve their luminescent properties and to meet the development of different display and luminescence devices. Inorganic compounds doped with rare earth ions form an important class of phosphors as they possess a few interesting characteristics such as excellent chemical stability, high luminescence efficiency, and flexible emission colors with different activators. As a new green luminescent material,  $\text{LaPO}_4$  Ce, Tb phosphor has been widely studied since it was found by different preparation methods [1,2].

These phosphors are widely used in displays and lighting devices. The useful applications of rare earth element compounds, especially lanthanide phosphate doped inorganic materials, have been touched upon broadly [5]. Over the past a few years, they have been applied in many fields, such as optical display panels, cathode ray tubes, optoelectronic, sensitive device, electronic and plasma display panels due to their special chemical and physical properties. Various solution-phase routes, including solid state reaction, sol-gel, precipitation, water oil micro emulsion, polyol-mediated process, ultrasonification, hydrothermal, and mechanochemical method, have been tried to lower the reaction temperature and obtain high-quality  $\text{LaPO}_4$  based nanoparticles. However, the simple and mass fabrication of  $\text{LaPO}_4$  nanocrystals with narrow grain size distribution and uniform morphology still remains a challenge [3,4]. It appears that the best solution

both to control powder morphology and to produce low cost thin films is the use of soft chemistry routes. We adopted the standard solid state reaction technique to prepare  $\text{LaPO}_4$  with good morphologies and fine crystal structures, and its emission intensity of luminescence was also studied [5,6]. The present paper reports the Photoluminescence (PL) of the  $\text{LaPO}_4$  phosphor doped with Ce, Eu and Tb rare-earth ions with different emission and excitation wavelengths, the doping concentration of Eu, Tb and Ce are 0.5, 1, 2, 3, 4 and 5 molar percentages respectively.

In the trivalent rare earth ions, the luminescence arises mainly due to transitions within the 4f shell. The efficiency of emission depends on the number of electrons in the 4f shell. The  $\text{Tb}^{3+}$  ion has 8 electrons in the 4f shell, which can be excited in the 4f-5d excitation band. The electron in the excited  $4f^7 - 5d$  state remains at the surface of the ion and comes under the strong influence of the crystal field resulting in the splitting of the excitation band. The excitation Spectra thus has multiple peaks. The excited ion in the  $4f^7 - 5d$  state decays stepwise from this state to the luminescent levels  $^5\text{D}_4\text{F}_3$  or  $^5\text{d}_4\text{F}_4$  by giving up phonons to the lattice. Luminescence emission occurs from either of these states, with the ion returning to the ground state. The emission line in the green region lying at 545 nm is due to the transition  $^5\text{D}_4 - ^7\text{F}_5$ . There are in fact multiple emission lines at each of these due to the crystal field splitting of the ground state of the emitting ions [7,8].

## 2. MATERIALS AND METHODS

All the chemical reagents were analytically pure and used without further purification.  $\text{LaPO}_4$  phosphor doped with Eu, Tb and varying concentrations of Ce (0.5, 1.0, 1.5, 2.0, 3.0, 4.0 and 5.0 mol %) rare-earth ions prepared using solid state diffusion reaction method. Stoichiometric proportions of raw materials namely, Lanthanum Oxide ( $\text{La}_2\text{O}_3$ ), Diammonium Hydrogen Phosphate  $[(\text{NH}_4)_2 \text{HPO}_4]$ , Cerium Oxide ( $\text{CeO}_2$ ), Europium Oxide ( $\text{Eu}_2\text{O}_3$ ) and Terbium Oxide ( $\text{Tb}_4\text{O}_7$ ) of assay 99.9% were used as starting materials and grinded in an agate motor and pestle, mixed and compressed into a alumina crucible and heated at  $1200^\circ\text{C}$  for 3 hours with heating rate of  $5^\circ\text{C}/\text{min}$  in the muffle furnace [9, 10]. The prepared samples were again grounded in to powder for taking the characteristic measurements.

All the phosphor samples were characterized by X-ray diffraction (Synchrotron Beam Indus -II), The Photoluminescence (PL) emission and excitation spectra were measured by Spectrofluorophotometer (SHIMADZU, RF-5301 PC) using 150 watts Xenon lamp as excitation source. The emission and excitation slit were kept at 1.5 nm, and recorded at room temperature. The Infrared spectra for the prepared solid nano powders were recorded in the range between  $400$  and  $4000\text{ cm}^{-1}$  on a Fourier transform spectrometer. The particle morphology of the phosphor was characterized by SEM.

## 3. RESULTS AND DISCUSSION

### 3.1 X-ray Diffractometry (XRD)

The crystallinity and phase purity of the phosphors were firstly examined by XRD analysis. fig.1 shows the typical X-ray diffraction (XRD) patterns of synthesized samples of  $\text{LaPO}_4$  doped with Eu(0.5),Tb(1.0) and Ce(2.0 mol%). The XRD patterns of the phosphor is in good agreement with the values from JCPDS no.35-731 of  $\text{LaPO}_4$ , which conform the phosphor is in monazite  $\text{LaPO}_4$  with monoclinic structure. All diffraction patterns were obtained using  $\text{CuK}\alpha$  radiation ( $\lambda = 1.540598\text{ \AA}$ ) at 40 kv and 30 mA, and divergence slit fixed at 1.52 mm. Measurements were made from  $2\theta = 15^\circ$  to  $50^\circ$  with steps of  $0.008356^\circ$ . When crystallites are less than approximately 100 nm in size, appreciable broadening in X-ray diffraction lines occurs. The crystallite size of powder sample were calculated by using Scherer equation  $D = 0.9 \lambda / \beta \cos\theta$  Where  $\beta$  represents full width at half maximum (FWHM) of XRD lines (0.112),  $\lambda$  = Wavelength of the X-rays.(0.154 nm in the present case),  $\theta$  = Braggs angle of the XRD peak. The calculated crystallite size for  $\text{LaPO}_4$ : Eu (0.5), Tb(1.0)&Ce(2.0mol%) phosphors is 73.14 nm, and from the XRD study it conforms the formation of phosphor in single phase and matched with JCPDS card no 35-731 of  $\text{LaPO}_4$ .

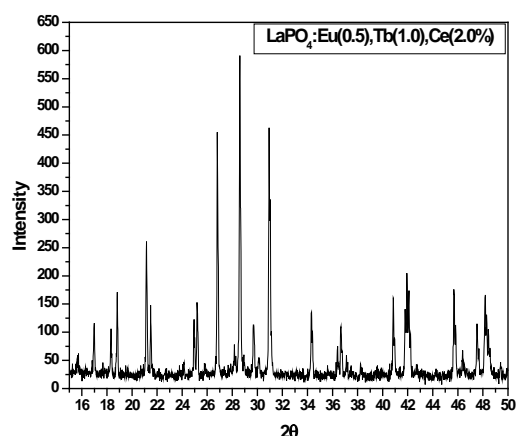


Fig.1: XRD of  $\text{LaPO}_4$  doped with  $\text{Eu}^{3+}$ ,  $\text{Tb}^{3+}$  and  $\text{Ce}^{3+}$

### 3.2 SEM Study:

Figure 2 and 3 show SEM image of  $\text{LaPO}_4$ : Eu (0.5), Tb (1.0), Ce(2.0 mol%). From SEM images it is observed that the particles look irregular shape and agglomerated having particle size of 1 micron to 5 microns.

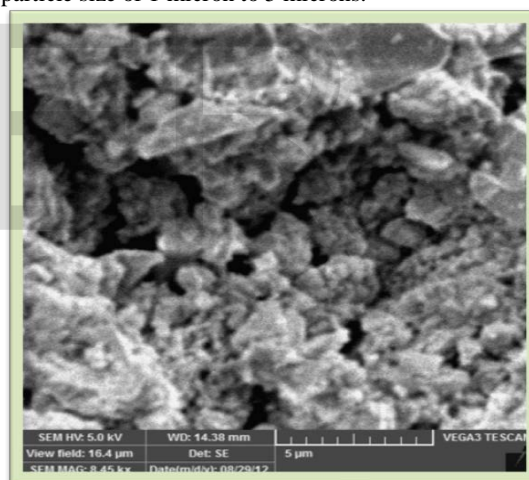


Fig.2. SEM Image of  $\text{LaPO}_4$ : Eu, Tb, Ce.(8.45 KX)

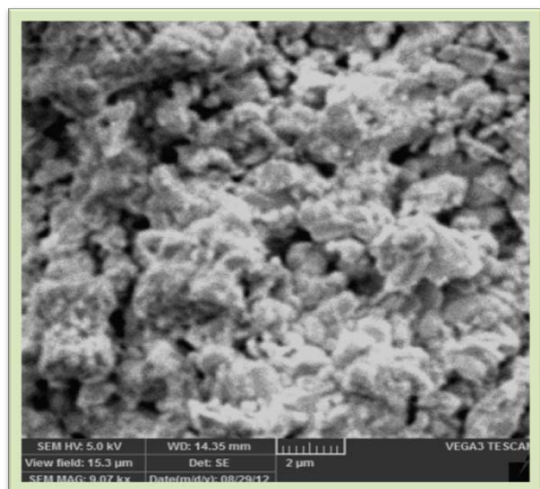
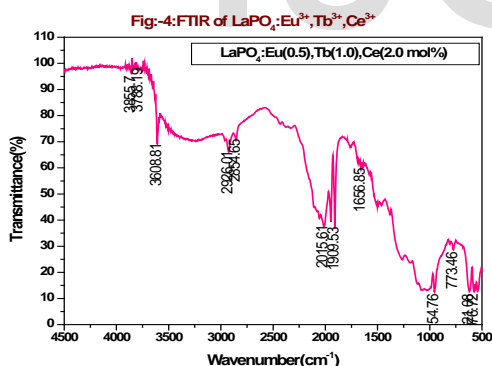


Fig.3. SEM Image of LaPO<sub>4</sub>: Eu, Tb, Ce.(9.07 KX)

### 3.3 FTIR study of LaPO<sub>4</sub>: Eu, Tb, Ce.

In order to determine the chemical bonds of the present studied phosphor FTIR analysis was carried out. Figure - 4 is the FTIR of the Eu, Tb and Ce doped LaPO<sub>4</sub> phosphor, the main absorption around 3600 are assumed H-O-H stretching followed by other bonds of C-H bending, C-O stretching and CO-OH stretching. CO-OH and H-O-H stretching are due to absorbed CO<sub>2</sub> and H<sub>2</sub>O molecules from atmosphere.

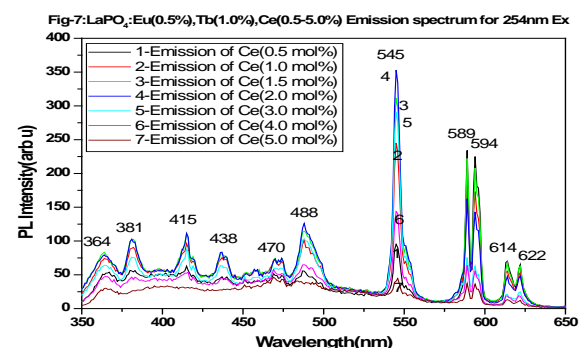
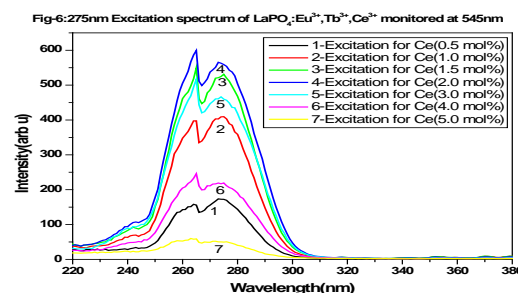
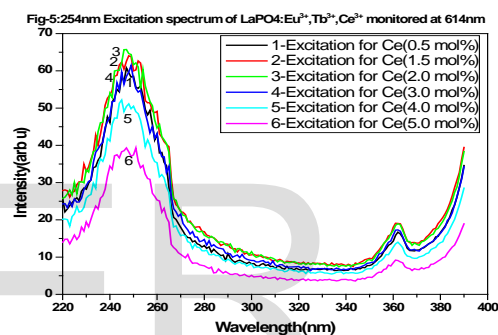


### 3.4 Photoluminescence Study:

Figure 5 and 6 are the excitation spectra of LaPO<sub>4</sub> doped with Eu(0.5), Tb(1.0) Ce (0.5 to 5%) when monitored at 614 and 545nm. From figure 6 it is observed that the excitation spectra consist of two absorption maxima at 264 and 275nm. Fig.7,8, 9, 10 and 11 are the emission spectra of LaPO<sub>4</sub> doped with Eu(0.5), Tb(1.0) and Ce(0.5,1.0,1.5,2.0,3.0,4.0 and 5.0 mol%) phosphor under different excitations at 254 and 275 nm wavelengths. The phosphor shows the PL peaks at 364, 381, 415, 438, 470, 488, 545, 589, 594, 614 and 622 nm with good intensity.

The excitation spectrum monitored with the emission of Tb<sup>3+</sup> (545 nm) consists of a broad band peaking at 275 nm with two shoulders at 241, 264 nm, which correspond to the transitions from the ground state <sup>2</sup>F<sub>5/2</sub> of Ce<sup>3+</sup> to the different components of the excited Ce<sup>3+</sup> 5d states split by the crystal field [22]. Excitation into the Ce<sup>3+</sup> band at 290 nm yields both the weak 5d-4f emission of Ce<sup>3+</sup> (300-400 nm) and the strong emission of Tb<sup>3+</sup> (488, 545, 583 and 622 nm, corresponding to <sup>5</sup>D<sub>4</sub>-<sup>7</sup>F<sub>6,5,4,3</sub> respectively), as shown in Fig. 6b. This indicates that an efficient energy transfer from Ce<sup>3+</sup> to Tb<sup>3+</sup> occurs in LaPO<sub>4</sub> doped with Eu(0.5), Tb(1.0) Ce (2) phosphor particles, as reported previously[11,12].

From the emission figures, as increase the excitation wavelength from 254 to 275nm, the emission peaks intensities decreased except 488 and 545 nm peaks, the intensity of 488 nm peak slightly increased and 545nm peak intensity is increased by two times which is shown in fig. 13 and table-3 for better comparison.



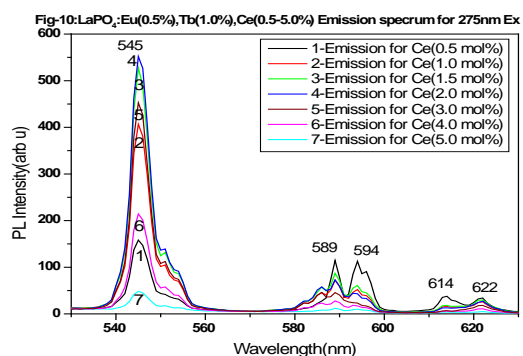
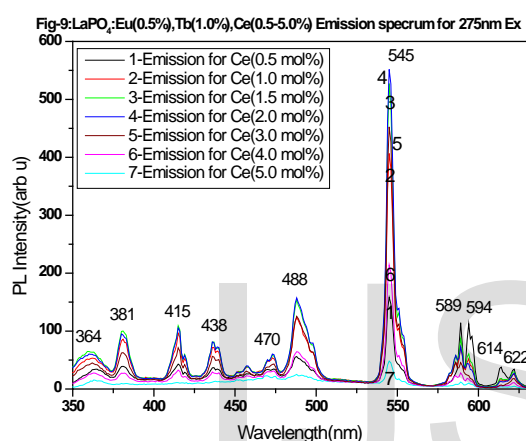
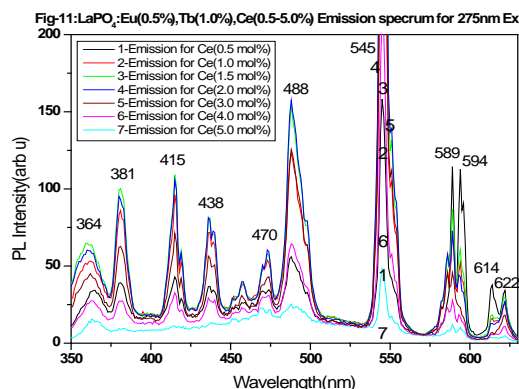
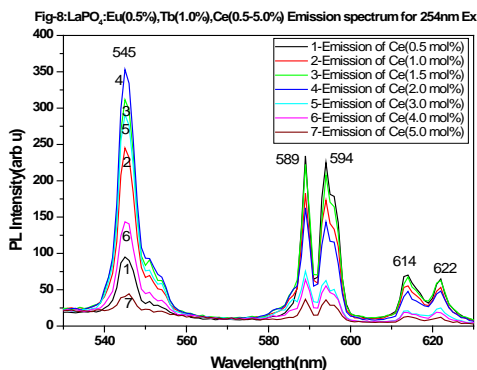


Fig-7,8 are the emission spectrum of  $\text{LaPO}_4:\text{Eu}(0.5),\text{Tb}(1.0)$  and  $\text{Ce}(0.5,1.0,1.5,2.0,3.0,4.0,5.0 \text{ mol\%})$  under 254nm excitation wavelength. From the graphs it is observed that the peaks at 364,381,415,438,470, 614,622nm with lower intensity and 488,545,589 and 594nm are with high intensity. As increasing the Ce concentration in  $\text{LaPO}_4:\text{Eu}(0.5),\text{Tb}(1.0)$  from 0.5 to 5.0 mol %, the 545nm peak intensity increases up to 2.0 mol% of Ce doping further increasing the Ce concentration the 545nm peak intensity gradually decreases. When concentration of Ce is more than 2.0 mol% in  $\text{LaPO}_4:\text{Eu}(0.5),\text{Tb}(1.0)$  the quenching effect started and maximum quenching at 5% of Ce ions in  $\text{LaPO}_4:\text{Eu}(0.5),\text{Tb}(1.0)$  is observed. The other major peaks at 589nm and 594nm peaks intensity is gradually decreases as Ce concentration increases and the remaining peaks at 364nm,381nm,415nm,438nm and 470nm peaks intensity increases as Ce concentration increases up to 1.5 mol% and further increase of Ce decreases the PL intensity .

Fig-9,10,11 are the emission spectrum of  $\text{LaPO}_4:\text{Eu}(0.5),\text{Tb}(1.0)$  and  $\text{Ce}(0.5,1.0,1.5,2.0,3.0,4.0,5.0 \text{ mol\%})$  under 275nm excitation wavelength. The same PL pattern is observed like 254nm excitation except the emission intensity of 545nm increases by 60% when compared to 254nm excitation when the Ce concentration is at 2%. However as Ce concentration increases the PL peak intensities of 364nm, 381nm, 415nm, 438nm and 470nm peaks increase marginally as Ce concentration increases up to 1.5 mol% and further decreased their intensity when excited with 275nm. Table-1 and Table-2 are the emission intensities of various peaks, they are observed in  $\text{LaPO}_4:\text{Eu}(0.5),\text{Tb}(1.0)$  and Ce for different concentrations when excitation with 254 and 275nm. The same is shown in fig-12 for better comparison.

It is clearly observed that the PL emission intensity of 545nm, 589nm and 594nm peaks are affected with respect to excitation wavelengths, which is as shown in fig-13. From the figure 545nm peak's intensity increased and 589nm, and the 594nm peak's intensity decreased as increasing excitation wavelengths. Table-3 gives the emission peak intensity for better comparison.

**Table-1**

S N o	Peak wavele ngth(n m)	Emission Intensity for different Ce concentrations under 254nm Excitation						
		0.5 %	1.0 %	1.5 %	2.0 %	3.0 %	4.0 %	5.0 %
1	364	54	75	84	80	66	48	31
2	381	58	91	103	102	77	47	25
3	415	64	96	113	112	88	54	32
4	438	48	75	82	85	65	45	30
5	470	51	70	74	73	60	57	46
6	488	56	101	115	126	10	65	39
7	545	96	246	312	354	293	143	45
8	589	234	182	222	163	753	64	37
9	594	225	173	208	143	633	55	36
10	614	70	55	68	48	21	18	14
11	622	65	53	63	48	25	19	12

Table-1 : Emission intensity for different peaks of  $\text{LaPO}_4:\text{Eu}(0.5),\text{Tb}(1.0)$  and  $\text{Ce}(0.5,1.0,1.5,2.0,3.0,4.0,5.0 \text{ mol}\%)$  under 254nm Excitation.

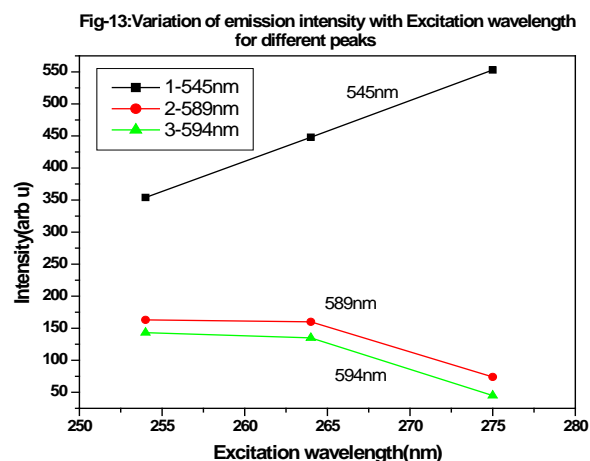
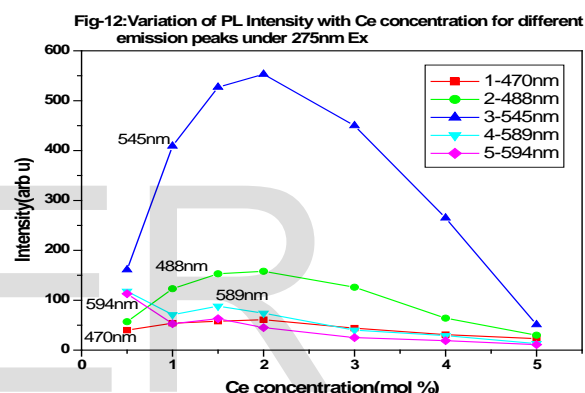
Table-2 : Emission intensity for different peaks of  $\text{LaPO}_4:\text{Eu}(0.5),\text{Tb}(1.0)$  and  $\text{Ce}(0.5,1.0,1.5,2.0,3.0,4.0,5.0 \text{ mol}\%)$  under 275nm Excitation

**Table-2**

S No	Peak wavelen gth(nm)	Emission Intensity for different Ce concentrations under 275nm Excitation						
		0.5 %	1.0 %	1.5 %	2.0 %	3.0 %	4.0 %	5.0 %
1	364	35	54	66	60	45	27	16
2	381	40	86	101	96	62	28	11
3	415	43	97	109	107	72	33	12
4	438	37	72	81	82	57	30	14
5	470	40	54	58	61	44	31	23
6	488	57	123	153	158	126	64	30
7	545	161	409	527	553	450	265	51
8	589	118	71	88	74	40	29	13
9	594	113	53	63	45	25	19	11
10	614	38	16	21	14	8	7	6
11	622	35	26	31	27	19	12	7

S No	Peak Wavelength(nm)	Emission peak intensity for different Excitation wavelengths		
		254nm	264nm	275nm
1	364	80	71	60
2	381	102	95	96
3	415	112	108	107
4	438	85	86	82
5	470	73	72	61
6	488	126	146	158
7	545	354	448	553
8	589	163	160	74
9	594	143	135	45
10	613	48	43	14
11	622	48	51	27

Table-3: Emission peaks intensity for different Excitation wavelengths of  $\text{LaPO}_4:\text{Eu}(0.5),\text{Tb}(1.0)$  and  $\text{Ce}(2.0 \text{ mol}\%)$



The excitation spectra of  $\text{LaPO}_4:\text{Eu}, \text{Tb}, \text{Ce}$  phosphor was recorded by monitoring the  $^5\text{D}_0 \rightarrow ^7\text{F}_2$  transition of  $\text{Eu}^{3+}$  at 614nm is shown in Fig. 5. The excitation spectra show broad absorption peak in the range 220-270nm. The



prominent excitation band was observed at 254nm due to the transition of  $\text{Eu}^{3+}$  and this clearly indicates that in  $\text{LaPO}_4:\text{Eu}, \text{Tb}, \text{Ce}$  phosphor where in Eu stabilized as  $\text{Eu}^{3+}$  ion. Fig. 7 and 9 are the emission spectra of  $\text{LaPO}_4:\text{Eu}, \text{Tb}, \text{Ce}$  phosphor at room temperature having 254 and 275nm excitation

Emission spectrum consists of emission peaks in the range of 550–650 nm, which result from  $^5\text{D}_0 \rightarrow ^7\text{F}_J$  ( $J=1, 2$ ) transitions of  $\text{Eu}^{3+}$  ion respectively. For an excitation wavelength of 254nm, the emission spectrum of  $\text{LaPO}_4:\text{Eu}, \text{Tb}, \text{Ce}$  consists of sharp emission lines at 589, 594, 614 and 622nm. The emission at 589nm and 594 nm originates from the allowed magnetic dipole (MD) transition  $^5\text{D}_0 \rightarrow ^7\text{F}_1$ . The  $^5\text{D}_0 \rightarrow ^7\text{F}_1$  magnetic dipole transition emissions are split at 589 nm and 594 nm. The peak was observed at 614nm due to the electric dipole  $^5\text{D}_0 \rightarrow ^7\text{F}_2$  transition, which has the less emission intensity. From the emission spectrum it is clearly observed that the emission intensity of magnetic dipole was higher than that of electric dipole transition, due to this  $\text{Eu}^{3+}$  ions occupy a low symmetry site in  $\text{LaPO}_4:\text{Eu}, \text{Tb}, \text{Ce}$  host. Both magnetic dipole transition and electric dipole transitions are shown in the emission spectra. If the magnetic dipole transition  $^5\text{D}_0 \rightarrow ^7\text{F}_1$  having the highest intensity then  $\text{Eu}^{3+}$  ions in host lattice occupies an inversion centre [15,17]. If the emission intensity of magnetic dipole transition was lower than that of electric dipole transition, which indicates that  $\text{Eu}^{3+}$  ions occupied without an inversion symmetric centers in the host.

The excitation spectra of  $\text{LaPO}_4:\text{Eu}, \text{Tb}, \text{Ce}$  extended from 250–280nm when monitored at 545nm which is shown as 6. The emission transitions in the wavelength range of 320–400 nm are characteristic of forbidden 4f-4f transitions within the  $\text{Tb}^{3+}$  configuration. The peaks with the position from 300 to 400 nm belong to the transitions between energy levels of the 4f<sup>8</sup> configuration of  $\text{Tb}^{3+}$  (f-f transitions)[16,18]. Among these, the 381 nm transition has the maximum intensity compared to the other transitions.

The emission spectra of  $\text{LaPO}_4:\text{Eu}, \text{Tb}, \text{Ce}$  phosphors ( $x = 0.5$ –5mol %) are compared in fig. 7,8,9,10,11. Each spectrum could be divided into two parts. The emission between 400–450 nm is due to transitions from the  $^5\text{D}_3$  excited state. Above 480–630nm, the emission peaks are originated from  $^5\text{D}_4$  excited states of  $\text{Tb}^{3+}$ . The  $^5\text{D}_4 \rightarrow ^7\text{F}_J$  ( $J = 6, 5, 4, 3$ ) characteristic emissions of  $\text{Tb}^{3+}$ , at 415, 438, 488, 545 and 622 nm, correspond to the transitions of  $^5\text{D}_3$  to  $^7\text{F}_5$ ,  $^7\text{F}_4$  and  $^5\text{D}_4$  to  $^7\text{F}_6$ ,  $^7\text{F}_5$ , and  $^7\text{F}_3$ , respectively. Under an ultraviolet lamp a strong greenish yellow luminescence is observed. The corresponding emission spectra of  $\text{LaPO}_4:\text{Eu}, \text{Tb}, \text{Ce}$  indicate narrow emissions which arise from 4f-4f transitions within  $\text{Tb}^{3+}$  ions as shown in fig.9. Among the measured emission transitions, the green-emission transition  $^5\text{D}_4 \rightarrow ^7\text{F}_5$  at 545 nm has more intense in nature due to the nature of the dopant  $\text{Tb}^{3+}$  ion in the host matrix. Emission intensities from  $^5\text{D}_3$  excited state decrease with the increase of the cerium concentration and show a maximum intensity at 545 nm when Ce is 2% when excited with 275nm. Comparing the emission intensities of

the different doping concentrations of Ce, it can be observed that in the range of 0.5 – 5 mol% for doping concentrations the luminescent intensities originating from the  $\text{Tb}^{3+}$ ,  $^5\text{D}_4 \rightarrow ^7\text{F}_J$  ( $J = 6, 5, 4, 3$ ) transitions increase with the increase of concentration, as a result, the luminescent intensity reaches maximum at 2 mol% of  $\text{Ce}^{3+}$ . When the concentration of  $\text{Ce}^{3+}$  increases more than 2 mol%, emission intensity decreases which is due to the concentration quenching and also Ce may be stabilizing in  $\text{Ce}^{4+}$  state. The decrease in the intensity with an increase in concentration was presumably due to the well-established theory of concentration quenching [9]. It can be seen from fig.9, a prominent and significant greenish yellow emission has been noticed for 1 mol%  $\text{Tb}^{3+}$ , which implies that this concentration in  $\text{LaPO}_4:\text{Eu}, \text{Tb}, \text{Ce}$  phosphor could be found as a potential and efficient phosphor for decorative CFL lamps.

The absorption band of  $\text{Ce}^{4+}$  is expected to be an efficient killer. Therefore, it is likely that  $\text{Ce}^{4+}$  is present in the  $\text{LaPO}_4:\text{Eu}, \text{Tb}, \text{Ce}$  lattice when the Ce concentration is more than 3%. The absorption band of  $\text{Ce}^{4+}$  is ascribed to a second phase containing  $\text{Ce}^{4+}$ . The  $\text{Ce}^{3+}$  emission in  $\text{LaPO}_4$  is double band, peaking at 250 and 275 nm, respectively resulting from the splitting of the ground states  $^2\text{F}_{5/2}$  and  $^2\text{F}_{7/2}$ . It is assumed that the cerium atoms have a good random distribution in the crystals, the inter-distance between  $\text{Ce}^{3+}$  and  $\text{Ce}^{4+}$  should also be in this range. It is known that the energy transfer between  $\text{Ce}^{3+}$  in  $\text{LaPO}_4$  is through dipole-dipole interaction [5].

Based on the above discussions, we may conclude that the  $\text{Ce}^{4+}$  is an efficient killer for the  $\text{Ce}^{3+}$  emission and does play an important role in the luminescence process of  $\text{LaPO}_4:\text{Eu}, \text{Tb}, \text{Ce}$ . Since the energy transfer between  $\text{Ce}^{3+}$  and  $\text{Ce}^{4+}$  is an inter-valance charge transfer, the efficiency of this energy transfer depends not only on the concentration of the  $\text{Ce}^{4+}$  but also on the special distribution of the cerium atoms in the material. The energy transfer between  $\text{Ce}^{3+}$  and  $\text{Ce}^{4+}$  reduces the energy transfer probability between  $\text{Ce}^{3+}$  and  $\text{Tb}^{3+}$ , and subsequently reduces the emission intensity of  $\text{Tb}^{3+}$ . The transfer of energy from sensitizer to an activator occurs without the appearance of a photon and is the primary result of the multipole interactions between the sensitizer and activator [19, 20].

The Cerium emission  $5d(^2\text{D}_{3/2}) \rightarrow 4f(^2\text{F}_{7/2} \text{ and } ^2\text{F}_{5/2})$  involves pure electric dipole transitions but  $4f \rightarrow 4f$  transitions in  $\text{Tb}^{3+}$  and  $\text{Eu}^{3+}$  have simultaneously a dipolar and a quadric polar character. Therefore two possible transfer mechanisms for  $\text{Ce}^{3+} \rightarrow \text{Tb}^{3+}$  energy transfer are dipole-dipole and dipole-quadrapole interactions may be present. In double phosphates, the presence of  $\text{PO}_4^{3-}$  groups, in which P-O bonds are strongly covalent, leads to relatively weak crystal field at the rare earth sites. The covalent nature of Ce-O bond is sufficient to shift the  $\text{Ce}^{3+}$  emission in these phosphates towards the higher wavelength. This results are in overlapping of  $\text{Ce}^{3+}$  emission (330–470 nm) and  $\text{Tb}^{3+}$  excitation (250–290) spectrum. Thus, it is possible to sensitize  $\text{Tb}^{3+}$  emission by  $\text{Ce}^{3+}$  emission. We got a strong intensity for  $^5\text{D}_4 \rightarrow ^7\text{F}_5$

emission line of  $Tb^{3+}$  ions in  $LaPO_4$ : Eu(0.5%), Tb(1%), Ce (2%)[22,23].

From the above graphs it is observed that many peaks are with less intensity at 364,381,415,438,470,614,622nm and with good intensity 488,545,589,594nm. Out of these the two peaks at 364 and 470nm are due to electron transitions of  $Ce^{3+}$ ,  $^2D_{3/2}(5d) \rightarrow ^2F_{5/2}(4f)$  (364nm) and  $^2D_{3/2}(5d) \rightarrow ^2F_{7/2}(4f)$  (470nm). The peaks at 381,415,438,488 545 and 622nm are due to electron transitions of  $Tb^{3+}$ , these are  $^5D_3 \rightarrow ^7F_J$  ( $J=6,5,4$ ),  $^5D_3 \rightarrow ^7F_6$ ,  $^5D_3 \rightarrow ^7F_5$ ,  $^5D_3 \rightarrow ^7F_4$  and  $^5D_4 \rightarrow ^7F_J$  ( $J=6,5,4$ ),  $^5D_4 \rightarrow ^7F_6$ ,  $^5D_4 \rightarrow ^7F_5$ ,  $^5D_4 \rightarrow ^7F_4$  respectively. The emission peaks at 589 and 594nm are due to magnetic dipole component of  $Eu^{3+}$  transition of  $^5D_0 \rightarrow ^7F_1$  and the PL emission peak at 614nm is due to electric dipole component of  $Eu^{3+}$  transition of  $^5D_0 \rightarrow ^7F_2$ . Among these emission transitions, the green emission transition  $^5D_4 \rightarrow ^7F_5$  at 545nm has been more intense due to the nature of the dopant  $Tb^{3+}$  ion in the host matrix, the red emission transition  $^5D_0 \rightarrow ^7F_1$  at 589 and 594nm have more intense due to the nature of the dopant  $Eu^{3+}$  in the host matrix [21,23]. The presence of Eu (0.5%) in  $LaPO_4$ : Tb (1%), Ce(2%) sensitizes the basic emissions of  $Tb^{3+}$  as well as emits its own emissions in  $Eu^{3+}$  state. The PL characteristics are concern the present studied phosphors can be used as phosphor in CFL's. Because the results obtained are comparable with the commercially available phosphors.

## CONCLUSION:

$LaPO_4$ : Eu, Tb, Ce phosphors were successfully synthesized by using solid state diffusion reaction method at low temperature. The main peak in XRD pattern was found around  $28.6^\circ$  corresponding to a d- value of about 3.15Å, followed by other less intense peaks corresponds to the monoclinic system of crystal structure of Lanthanum Phosphate. The calculated crystallite size for  $LaPO_4$ : Eu(0.5),Tb(1.0) & Ce(2.0mol%) phosphors is 73.14 nm, and from the XRD study it conforms the formation of phosphor is mostly in single phase. This method is easy for the preparation of Eu, Tb and Ce doped  $LaPO_4$  phosphors and can be potentially applied to the synthesis of other high quality rare earth ions doped phosphate phosphor materials with micro/nano structure.  $LaPO_4$ : Eu, Tb, Ce phosphor powder was successfully synthesized using a modified solid state method.  $LaPO_4$ : Eu, Tb, Ce phosphor shows green, orange-red emission under 254nm excitation. The photoluminescence study shows that the emissions from electric dipole transition ( $^5D_0 \rightarrow ^7F_2$ ) is less over that of magnetic dipole transition ( $^5D_0 \rightarrow ^7F_1$ ). The optimum concentration of  $Eu^{3+}$  in  $LaPO_4$ : Eu, Tb, Ce was 2 mol%. The PL spectra also show a strong emission at 545nm ( $^5D_4 \rightarrow ^7F_5$ ) of  $Tb^{3+}$ . The  $LaPO_4$ : Eu, Tb, Ce phosphors can be easily applied in various types of lamp and display due to its good PL performance. The results indicated that present phosphor could find application in white light emitting CFLs.

## References:

[1] Mounir Ferhi, Karima Horchani-Naifer, Mokhtar Ferid, Combustion synthesis and luminescence properties of  $LaPO_4$ : Eu (5%)

Journal of Rare Earths, Vol. 27, No. 2, Apr. 2009, p. 182.

[2] Stouwdam J W, Hebbink G A, Huskens J, Veggel F C JM van, Lanthanide-doped nanoparticles with excellent luminescent properties in organic media. Chem. Mater., 2003, 15: 4604.

[3] Albrand K R, Attig R, Fenner J, Jesser J P, Moot D. Crystal structure of the laser material  $NdP_5O_{14}$ . Mater. Res. Bull., 1974, 9: 129.

[4] Buisette V, Moreau M, Gacoin T, Boilot J P, Chane-Ching J. Y, Le Mercier T. Colloidal synthesis of luminescent rhabdophane,  $LaPO_4:Ln^{3+} \cdot xH_2O$  ( $Ln=Ce, Tb, Eu$ ;  $x \approx 0.7$ ) nanocrystals. Chem. Mater., 2004, 16: 3767.

[4] Kang Y C, Kim E J, Lee D Y, Park H D. High brightness  $LaPO_4$ : Ce,Tb phosphor particles with spherical shape. J. Alloys Compd., 2002, 347: 266.

[5] Rao R P, Devine D J. RE-activated lanthanide phosphate phosphors for PDP applications. J. Lumin., 2000, 87-89: 1260.

[6] Xiu Z, Liu S, Lü M, Zhang H, Zhou G. Photoluminescence of  $Eu^{3+}$ -doped  $LaPO_4$  nanocrystals synthesized by combustion method. Mat. Res. Bull., 2006, 41: 642.

[7] Gallini S, Jurado J R, Colomer M T. Combustion synthesis of nanometric powders of  $LaPO_4$  and Sr-substituted  $LaPO_4$ . Chem. Mater., 2005, 17: 4154.

[8] Schuetz P, Caruso F. Electrostatically assembled fluorescent thin films of rare-earth-doped lanthanum phosphate nanoparticles. Chem. Mater., 2002, 14: 4509.

[9] Page, P., Murthy, K.V.R. Luminescence associated with  $Eu^{3+}$  in two host lattices (2010) Philosophical Magazine Letters, 90 (9), pp. 653-662.

[10] Suresh, K., Murthy, K.V.R., Atchyutha Rao, C., Poornachandra Rao, N.V., Subba Rao, B. Synthesis and characterization of nano Sr  $2CeO_4$  doped with Eu and Gd phosphor (2013) Journal of Luminescence, 133, pp. 96-101.

[11] [12] Bril A, Wanmaker W L. Some properties of europium activated phosphors. J. Elec. Chem. Soc., 1964, 111(12): 1363.

[12] Yu L, Song H, Lu S, Liu Z, Yang L, Kong X. Luminescent properties of  $LaPO_4:Eu$  nanoparticles and nanowires. J. Phys.Chem., 2004, 108: 16697.

[13] Dexpert-Ghys J, Mauricot R, Faucher M D. Spectroscopy of  $Eu^{3+}$  ions in monazite type lanthanide orthophosphates  $LnPO_4$ ,  $Ln=La$  or  $Eu$ . J. Lumin., 1996, 69: 203.

[14] Rambabu U, Buddhudu S. Optical properties of  $LnPO_4:Eu^{3+}$  ( $Ln=Y, La$  and  $Gd$ ) powder phosphors. Opt. Mater., 2001, 17:404.

[15] Shionoya S, Yen W M. Phosphor Handbook, Phosphor Research Society, CRC Press, 1998, 459.

[16] Blasse G, Grabmeier BC. Luminescent Materials. New York: Springer-Verlag; 1994.

[17] Nazarov M V, Zamoryanskaya M V, Popovici E-J, Ungur L, Tsukerblat B S. Luminescence of calcium tungstate

- phosphors doped with europium and terbium.  
J. Mold. Phys. Sci., 2003,2(1): 68.
- [18] Brixner L H, Chen H Y. On the structural and luminescent properties of the  $M'$   $\text{LnTaO}_4$  rare earth tantalates. J. Electrochem.Soc., 1983, 130: 2435.
- [19] R.P. Rao,  $\text{Tm}^{3+}$  activated lanthanum phosphate: a blue PDP phosphor Journal of Luminescence 113 (2005) 271–278.
- [20] Kim G C, Mho S I, Park H L. Observation of energy transfer between  $\text{Ce}^{3+}$  and  $\text{Eu}^{3+}$  in  $\text{YAlO}_3:\text{Ce}$ , Eu. J. Mater. Sci. Lett., 1995, 14(11): 805.
- [21] Sohn K S, Choi Y Y, Park H D. Photoluminescence behavior of  $\text{Tb}^{3+}$  activated  $\text{YBO}_3$ , phosphors, J. Electrochem. Soc., 2000, 147(5): 1988.
- [22] Rap R P.  $\text{Tb}^{3+}$  activated green phosphors for plasma display panel application, J. J. Electrochem. S-III., 2003.150(8): H165.
- [23] R.P. Rao and D.J. Devine RE-activated lanthanide phosphate phosphors for PDP Applications, Journal of Luminescence 87-89 (2000) 1260-1263.

IJSER